PHYSICAL REVIEW B **73**, 045312 (2006)

Strain determination in MBE-grown InAs quantum wires on InP

A. Mazuelas,[1] L. González,[2] J. M. García,[2] Y. González,[2] T. Schuelli,[1] C. Priester,[3] and H. T. Metzger[1]
[1]*European Synchrotron Radiation Facility (ESRF), BP 220, F-38043 Grenoble, France*
[2]*Instituto de Microelectrónica de Madrid (CNM-CSIC), Isaac Newton 8, E-28760 Tres Cantos, Spain*
[3]*Institut d'Electronique, de Microélectronique et de Nanotechnologie, F-59652 Villeneuve d'Ascq, France*
(Received 28 June 2005; revised manuscript received 9 November 2005; published 12 January 2006)

We have determined the strain in the three crystallographic directions in InAs quantum wires (QWr) grown by molecular beam epitaxy on (001)InP substrate. We used triple crystal x-ray diffraction to make scans along and perpendicular to the QWr direction in reciprocal space, around InP(220) reflections. We use the shape and strain sensitivity of the different scans to deconvolute both contributions. We used the α_f scan analysis in grazing incidence diffraction to measure the strain relaxation perpendicular to the QWr as a function of height in the wire. We finally compare these results with finite elements calculations of the strain tensor in InAs QWr on InP.

DOI: 10.1103/PhysRevB.73.045312 PACS number(s): 68.65.La, 68.60.Bs, 81.07.Vb, 81.05.Ea

INTRODUCTION

In the last years, there has been a tremendous interest in systems of reduced dimensionality, especially on quantum wires (QWr) and quantum dots. These are being synthesized through strain-related self-organization phenomena,[1] or by lithographic techniques. The main advantages of self-organization versus lithographic growth techniques are lower defect density, higher yield (larger areas produced in less time), and nanometer scale confining dimension.

We have produced highly ordered arrays of self-assembled QWr-like structures of InAs on InP(001) by solid source molecular beam epitaxy (MBE).[2] The spontaneous formation of InAs QWr instead of Q dots, structures more efficient for strain relaxation, in exactly oriented InP(001) surface is due to the intrinsic strain asymmetry in ⟨110⟩ directions built in at the InAs/InP interface under V-element stabilized growth conditions. This asymmetry in strain leads to a faster relaxation along [110] with the subsequent formation of QWr nanostructures parallel to [1-10] direction.[3,4] Their size can be optimized for light emission at 1.55 μm wavelength.[5,6] The photoluminescence (PL) emission shows a strong polarization dependence with QWr direction. We observe[2] a higher PL intensity when the detector polarization is oriented parallel to [1-10], the wires axis. Furthermore, we have also observed strong optical anisotropy in the spectral region of the E_1 transition of InAs.[7] These results indicate an asymmetry in lateral carrier confinement, probably due to an asymmetric strain distribution related to the peculiar shape of these nanostructures. However, strain distribution inside the QWr is not well known. The aim of this paper is to obtain a map of the strain inside the self-assembled InAs QWr grown on InP.

EXPERIMENT

After oxide removal of the InP(001) substrate, a 2000 Å thick InP buffer layer was grown at a substrate temperature T_s=450 °C. The InP substrates were exactly oriented (001) (±0.1° according to commercial specifications). The InAs surface layer was grown at T_s=400 °C, at a growth rate of 0.44 monolayers per second (ML/s) and a beam equivalent pressure (BEP) $(As_4)=3\times10^{-6}$ mbar. After deposition of 2.5 ML of InAs, the growth was interrupted during 60 s and the substrate temperature was increased to 470 °C for QWr formation.

Grazing incidence diffraction (GID) was measured both with a point detector and with a linear position sensitive detector (PSD) at the Anomalous Scattering Beamline (ID01) of the ESRF. We have measured scans and reciprocal space maps around the {220} InP reflections, at an energy of 11.867 KeV. In order to be sensitive to the top-most layer, the measurements were performed at grazing incidence (α_i) and exit (α_f), slightly above the critical angle (α_c), which for InP is 0.26 deg.

RESULTS AND DISCUSSION

We have used atomic force microscopy (AFM), to characterize the surface morphology (Fig. 1). The QWr are formed along the [1-10] direction and have an average lateral periodicity of 200 Å. They are about 10–20 Å high and can reach up to 1 μm in length. According to AFM measurements, there is a height dispersion between different QWr of about 3 ML (considering 1 ML InAs is 3.02925 Å) around the average value. Along a single QWr we observe a dispersion in height of ±1 ML.

Triple crystal grazing incidence x-ray diffraction (GID) was used to determine the shape, lateral correlation, and strain in the directions parallel and perpendicular to the QWr.

X-ray scattering methods have proven to be an excellent tool to determine the size, shape, elastic strain, chemical composition, and positional correlation among the nanostructures. Beyond its sensitivity to deformation of the crystal lattice, it is sensitive to fluctuations of the surface and interface morphology on length scales ranging from 0.01 nm up to several micrometers. The main advantage of x-ray techniques is based on the high resolution in reciprocal space, which is a direct consequence of the high angular resolution of a few seconds of arc. Therefore, x rays are sensitive to

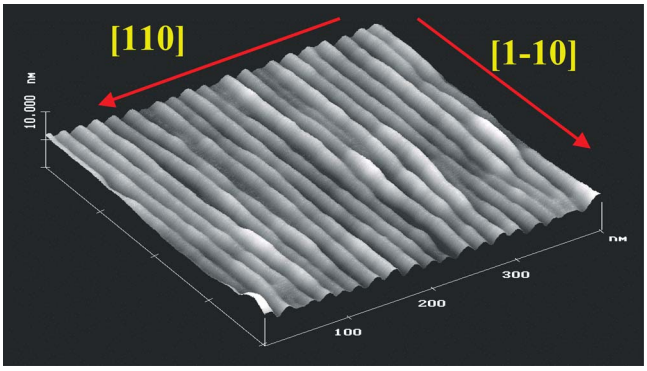

FIG. 1. (Color online) Atomic force microscopy (AFM) image of the surface of the studied sample showing the highly ordered arrays of self-assembled QWr-like structures of InAs on InP(001). The QWr are aligned parallel to the [1-10] direction. They are about 10–20 Å high and can reach up to 1 μm in length.

very small variations of lattice parameters. Moreover, thanks to the coherent lengths of typically a few micrometers, information on electron density fluctuations on a larger length scale than atomic spacings can be obtained. X rays interact weakly with matter, and, due to the small volume fraction of the mesoscopic structures, compared with the x-rays penetration depth, the scattering signal is very small, and has to be enhanced compared to the large signal from the underlying substrate. Therefore, surface and interface sensitive techniques, using grazing incidence geometry, and applying highly brilliant synchrotron radiation are among the most promising approaches. Combined with anomalous scattering close to the absorption edge of one of the constituent elements, adds chemical sensitivity to these techniques. Another advantage of x-ray techniques is that, being the spot size in the range of a few square millimeters, they statistically average over large ensembles of nanostructures. Previous to the present work, grazing incidence x-ray scattering techniques have been applied to InAs quantum dots on GaAs,[8,9], SiGe islands on Si,[10,11] and nitrides quantum dots.[12] A recent and complete review is presented in Ref. 13.

The scans performed in reciprocal space are shown schematically in Fig. 2. We have made radial and angular scans near the (220) and (2-20) reflections (marked 1–4 in Fig. 2). Angular scans contain information of the shape and lateral correlations of the QWr. The intensity in radial scans is, in addition, strain sensitive. Measuring angular and radial scans, both parallel ([1-10]) and perpendicular ([110]) to the QWr enables us to separate the shape, correlations and strain.

Figure 3 shows angular and radial scans close to (2-20) [Figs. 3(a) and 3(b)] and (220) [Figs. 3(c) and 3(d)] InP substrate reflections. The angular scan shown on Fig. 3(a), corresponding to a q_a variation in the direction perpendicular to the QWr, shows two peaks. The origin of these peaks is the lateral periodicity of the QWr. From the angular distance we can directly deduce a period D of the QWr array of 200 Å, in good agreement with AFM values. In order to extract more geometrical information, we have fitted the experimental intensity to the product of two functions describing the shape and the correlation of the QWr. As a first approximation a Gaussian function with dispersion σ is used as

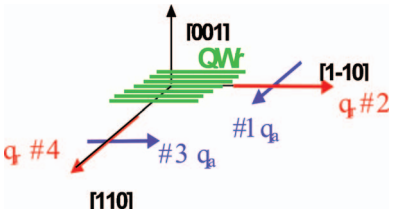

FIG. 2. (Color) Reciprocal space scheme, showing some of the different scans performed in this work. Scans 1 and 2 are, respectively, angular scan perpendicular to the QWr radial scan parallel to the QWr, performed around the (2-20) reflection of the InP(001) substrate. Scans 3 and 4 are, respectively, angular scan parallel to the QWr and radial scan perpendicular to the QWr passing through the (220) reflection of the InP(001) substrate. The radial scan perpendicular to the QWr (scan 4) is simulated (Fig. 6) in order to obtain the strain profile along the [110] direction.

shape function. The Gaussian profile was chosen for simplicity considering that, even if the profile is a truncated triangle, there is a dispersion of sizes in QWr height and width; the Gaussian envelope takes into consideration this dispersion. As correlation function, we have used[14]

$$\mathbf{C}(\mathbf{q_a}) = \frac{1 - \exp(-1/2\gamma^2 q_{\|}^2)}{1 + \exp(-1/2\gamma^2 q_{\|}^2) - 2\exp(-1/4\gamma^2 q_{\|}^2)\cos(\mathbf{D}q_{\|})},$$

which is appropriate for imperfect crystals. Here γ stands for the ordering parameter, $\mathbf{q}_{\|}$ is the lateral momentum transfer, and **D** is the average in-plane distance between adjacent InAs wires. The fit to the experimental curve is shown on Fig. 4. The resulting parameters are lateral period $D=190$ Å, QWr width $w=138$ Å, lateral correlation $\xi_H=2490$ Å (~13 periods), where the lateral correlation is in this model $\xi_H = D^3/\gamma^2$. Both D and w values are in agreement with AFM and TEM previous results.[5]

On the contrary, on the radial scan around the (2-20) reflection of InP, where q_r varies along the QWr axis [Fig. 3(b)], we only observe the Bragg peak corresponding to the InP substrate. This means that along the QWr, the InAs is fully strained to match the InP lattice parameter (5.8688 Å), corresponding to 3.2% misfit strain.

We have also made a reciprocal space map around the (2-20) InP reflection (Fig. 5). The (2-20) reflection of the InP substrate lays in the center. The vertical axis for $q_a=0$ corresponds to the radial scan shown in Fig. 3(b). The horizontal cut at the maximum intensity of such reflection corresponds to the angular scan represented in Fig. 3(b). By performing q_r scans passing through the correlation maxima at $q_a = \pm 0.035$ Å^{-1}, we can measure the width of the correlation peaks along the [1-10] direction. By application of Scherer's formula,[15] we obtain the QWr length to be 2000 Å. This value is smaller than that estimated by AFM and reflects the lack of uniformity in height inside a single QWr and the meandering of QWr direction.

We have also measured angular and radial scans around the (220) reflection of InP. Now, in the angular scan [Fig. 3(c)] q_a direction is parallel to the wires axis, while the q_r direction in the radial scan [Fig. 3(d)] is perpendicular to the QWr. In the q_a scan [Fig. 3(c)] we obtain a single peak with

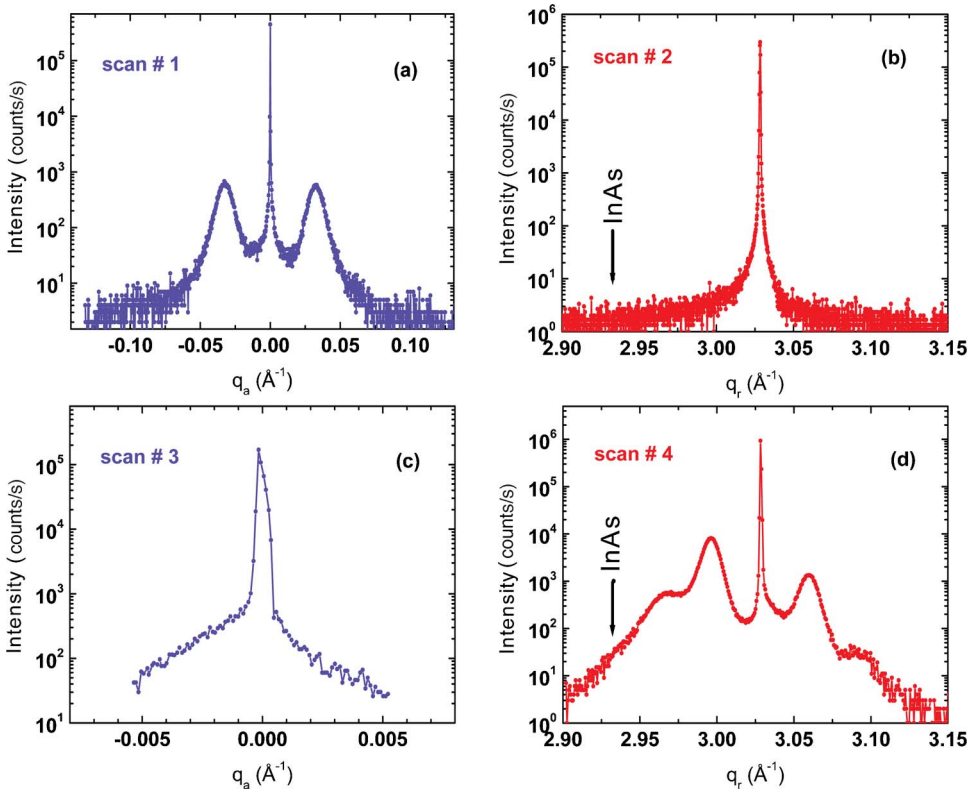

FIG. 3. (Color online) Angular and radial scans near the (220) and (2-20) reflections of InP(001) substrate (scans 1–4 in Fig. 2). Angular scans are sensitive to the shape and correlation, while radial scans are sensitive also to the strain.

no correlation or shape dependent intensity, which means that all QWr are elongated along the [1-10] direction. Although this result was already obtained by the AFM local measurement of surface morphology, x-ray diffraction (XRD) provides stronger statistical significance.

On the contrary, the radial scan with q_r perpendicular to the QWr direction [Fig. 3(d)] shows a rich peak structure with an intensity profile that is asymmetric with respect to the sharp substrate (220) peak, indicating strain relaxation toward the lattice parameter of InAs. In this case, the shape and correlation functions are modulated by the strain. In addition, we observe a strain-induced broadening of the intensity due to a lattice parameter distribution in the QWr. Therefore, our results show that the QWr are fully strained along [1-10] and there is a distribution of lattice parameters along [110], the short direction of the QWr. This variation of lattice parameter in [110] will induce a variation in lattice parameter from the bottom to the top of the QWr. In order to obtain more information about lattice parameter distribution inside the QWr, we have made simulations of the intensity distribution that are presented in Fig. 6.

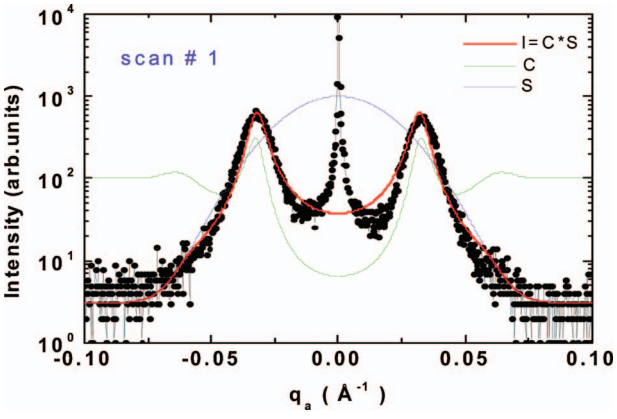

FIG. 4. (Color) The angular scan passing through the (2-20) reflection is analyzed as the product of the correlation and the shape functions. The results of the fit are lateral period=190 Å, QWr width=138 Å, and lateral correlation=2490 Å ~ 13 periods.

The simulations use the kinematical approximation and include a truncated-triangle section of the QWr formed by

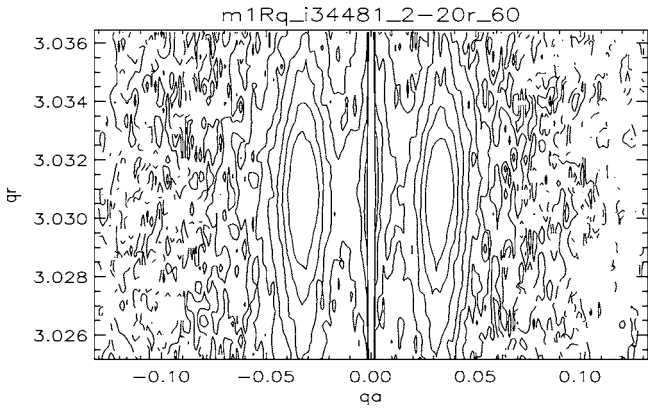

FIG. 5. Reciprocal space map around the InP(2-20) reflection. For clarity, we have shown only the diffracted intensity lower than 60% of the maximum of the InP peak. From this map we can obtain that: (a) all the InAs in the QWr has in the [1-10] direction the lattice parameter of the InP substrate, (b) the QWr have a length along the [1-10] direction of 2000 Å, obtained by the application of Scherer's formula (Ref. 15) to the width of the correlation maxima to the sides of the InP peak.

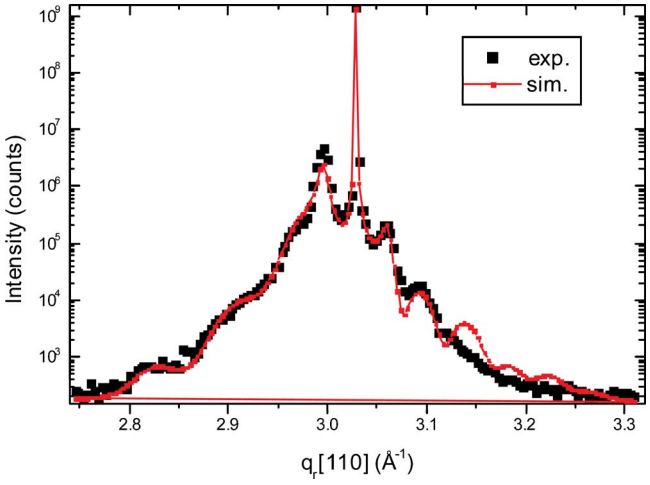

FIG. 6. (Color online) Comparison between the simulated and the experimental radial scan along the [110] direction passing by the (220)InP substrate reflection. From the simulation, a profile of the QWr strain along the [110] direction is obtained.

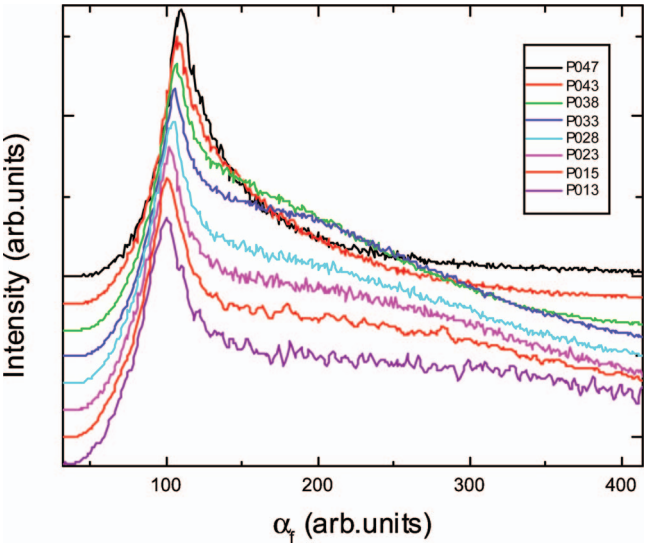

FIG. 7. (Color) Shift of the maximum of the α_f while scanning along q_r (scan 4 in Fig. 2(d) with recording of the α_f scan). According to Kegel *et al.* Refs. 8 and 9 the displacement of the maximum of α_f (normalized to the value of the critical angle α_c) is related to the height (z) for each q_r. On the other hand, q_r is directly related to the lattice parameter along the [110] direction.

lamellae of InAs with different strain in the vertical direction, and constant strain within the lamellae. Initial inputs of the simulation were the values on the morphology provided by AFM analysis, and the assumption than the InAs relaxes linearly from the QWr base, where it is deformed to match the InP lattice parameter, to its bulk value at the top of the wire. The best fit was obtained for a QWr base of 150 Å, a width at the top of 6 Å, and a lattice parameter equal to that of InP at the base, and of 5.9467 Å at the top. Once the other determinations of the strain were obtained (see below) the new values were crosschecked with this simulation method, in order to obtain a coherent model. The strong point of this method is the determination of the strain, with few assumptions. As one of its drawbacks, we would mention that slight differences with respect to the assumed linear relaxation have little influence on the fit to the diffraction curve. In order to determine if the main assumption of this model, the linear relaxation with height, is appropriate or not, we have used the method developed by Kegel *et al.*[8,9] We have measured the distribution of diffracted intensity as a function of exit angle (α_f), i.e. α_f scans were performed at different q_r along the radial axis crossing the InP(220) reflection. From the displacement of the maximum of α_f normalized to the value of the critical angle (α_c), Fig. 7, we have calculated the height (z) for each q_r. Since q_r is directly related to the lattice parameter, one obtains the relation between the lattice parameter along the [110] direction and the QWr height. The result of this measured relation is plotted in Fig. 8.

From the lattice parameter obtained, and considering pure InAs QWr, the strain is then calculated as a function of the height. The last assumption on the composition of the QWr relies on previous (DAFS) studies[16] where the P/As intermixing is limited to the first interface monolayer. With the measured strain in the [110] and [1-10] directions, one can calculate the strain in the [001] direction by applying elasticity theory. We then plot the three components of the strain as a function of z in Fig. 9. According to our results, this figure shows that the InAs has the lattice parameter of InP at the base of the wires, both in the [110] and [1-10] directions. In the [001] directions, it suffers the Poisson tetragonal elongation (calculated).

For increasing height (z), the InAs keeps the InP lattice parameter along the wires [1-10] direction, and relaxes progressively toward its own lattice parameter in the [110] direction. As seen in Fig. 8 (and Fig. 9), our results suggest that the relaxation of InAs in the [011] direction with height (z) is not linear, but changes its character after the first 2–3 monolayers (6–10 Å). The relaxation is slower initially, probably due to the influence of the substrate, and after a critical thickness, increases in the direction of the QWr top. In the [001] direction, the InAs also relaxes due to the reduction of strain in the [110] direction.

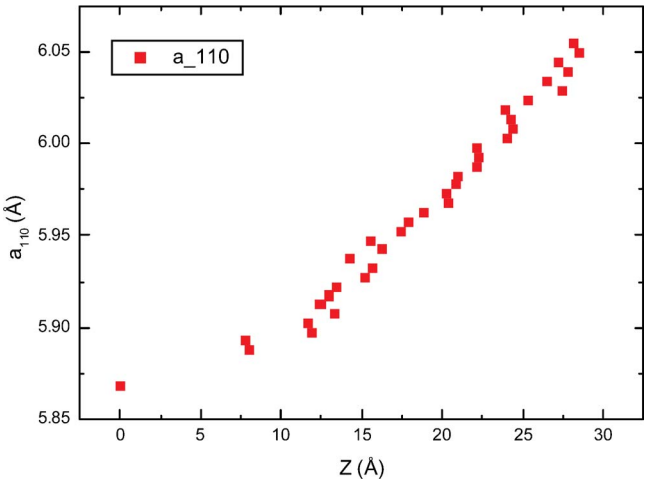

FIG. 8. (Color online) Measurement of the lattice parameter along the [110] direction for increasing z (height in the QWr), obtained from the shift of the α_f scan [Kegel's method (Refs. 8 and 9)].

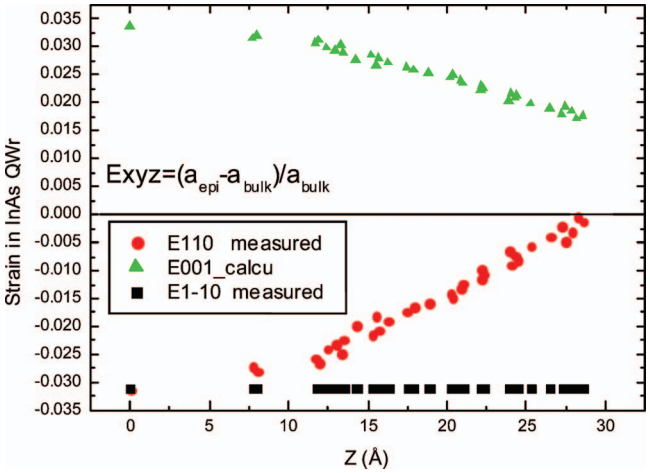

FIG. 9. (Color) Strain distribution along QWr height (E_{001}) obtained applying the elastic theory to the lattice parameters values along 110 and 1-10 (E_{110}, E_{1-10}) obtained by measuring XRD at grazing incidence. This model assumes a diagonal strain tensor, which is obviously a simplification. For a more realistic model, it is possible to use finite elements simulations (Fig. 10)

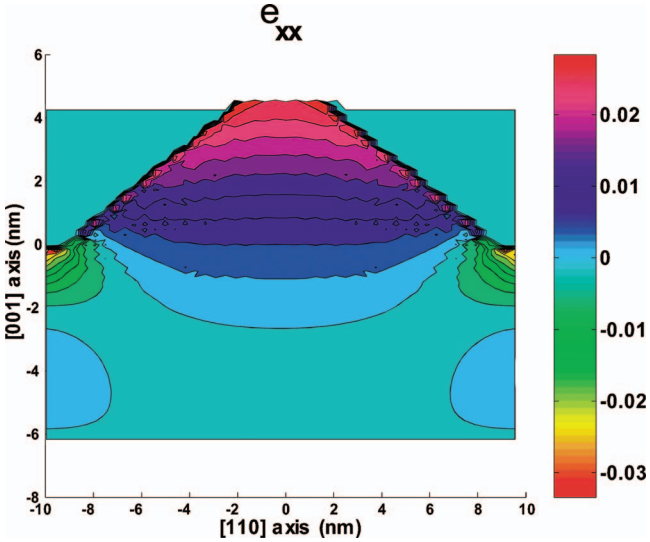

FIG. 10. (Color) Finite elements simulation of the vertical cross section of the QWr truncated triangle. The simulations yield a three-dimensional representation of the strain tensor, with nonzero off-diagonal strain values. We show only one of the two-dimensional maps for simplicity, with axis [110] (horizontal), and [001] (vertical). Note the important border and surface effects.

I. FINITE ELEMENTS/STRAIN SIMULATION

Finite difference method simulation was performed to map the strain produced by the InAs QWr (Fig. 10). We assume coherent growth of InAs on InP (no dislocation). We perform the finite difference method[17] in a 2D periodic frame, in the plane determined by the [110] and [001] crystal axes.

The previously determined values of the strain versus height has been used as input in the finite elements simulations. We obtained that an interface layer where intermixing of As and P is produced, forming an InAsP layer 2–3 monolayers thick, slightly improves the agreement. Actually, recent experimental results indicate that the interface layer is 2 ML thick.[4] We should be cautious in interpreting this result though, since the models are different and a direct comparison is not possible. Indeed our models for simulation of the strain obtained by GID (Fig. 6) and α_f shift (Fig. 7) techniques, both consider the QWr made of a vertical stack of horizontal lamellae of material where the strain is constant. This is clearly an oversimplification, since at the surface the strain must be different than inside the crystal. Opposite to these models, the finite element calculation renders more realistic strain distributions including border and surface effects (see Fig. 10). In Fig. 10, we show a map of the strain of InAs with respect to the InP substrate calculated for a [1-10] cross section of one QWr. In this figure, strain ϵ_{xx} along [110] is plotted versus QWr height. We observe that the InAs QWr is more coupled to the substrate in average that the value at the center (where the relaxation toward its bulk value is larger). Nevertheless, the measured strain distribution by GID is a good check of the validity of the finite element calculation.

SUMMARY

We have used complementary techniques such as grazing incidence diffraction scans, reciprocal space maps, the shift of the α_f scan, and finite element calculations to determine the strain status on InAs QWr grown by MBE on InP(001) substrates. We obtain that all the QWr are aligned along the [1-10] direction, that the InAs is in this direction elastically strained to match the InP substrate lattice parameter, while it relaxes nearly linearly with height along the [110] direction. As a result, there is a partial relaxation along the growth direction [001].

ACKNOWLEDGMENTS

This work was partially financed by Spanish MCyT under NANOSELF Project No. (TIC2002-04096) and by the SANDiE Network of excellence (Contract No. NMP4-CT-2004-500101 group TEP-0120).

[1] A. C. Chen, A. M. Moy, P. J. Pearah, K. C. Hsieh, and K. Y. Cheng, Appl. Phys. Lett. **62**, 1359 (1993).

[2] L. González, J. M. García, R. García, J. Martínez-Pastor, C. Ballesteros, and F. Briones, Appl. Phys. Lett. **76**, 1104 (2000).

[3] J. M. García, L. González, M. U. González, J. P. Silveira, Y. González, and F. Briones, J. Cryst. Growth **227/228**, 975 (2001).

[4] M. U. González, L. González, J. M. García, Y. González, J. P.

Silveira, and F. Briones, Microelectron. J. **35**, 13 (2004).
[5] D. Fuster, L. González, Y. González, J. Martínez-Pastor, Teresa Ben, Arturo Ponce, and Sergio I. Molina, Eur. J. Phys. **40**, 433 (2004).
[6] D. Fuster, M. U. González, L. González, Y. González, T. Ben, A. Ponce, S. Molina, and J. Martínez-Pastor, Appl. Phys. Lett. **85**, 1424 (2004).
[7] J. A. Prieto, G. Armelles, C. Priester, J. M. García, L. González, and R. García, Appl. Phys. Lett. **76**, 2197 (2000).
[8] I. Kegel, T. H. Metzger, P. Fratzl, J. Peisl, A. Lorke, J. M. García, and P. M. Petroff, Europhys. Lett. **45**, 222 (1999).
[9] I. Kegel, T. H. Metzger, A. Lorke, J. Peisl, J. Stangl, G. Bauer, J. M. Garcia, and P. M. Petroff, Phys. Rev. Lett. **85**, 1694 (2000); I. Kegel, T. H. Metzger, A. Lorke, J. Peisl, J. Stangl, G. Bauer, K. Nordlund, W. V. Schoenfeld, and P. M. Petroff, Phys. Rev. B **63**, 035318 (2001).
[10] M. Schmidbauer, M. Hanke, H. Raidt, R. Kohler, and H. Wawra, Phys. Rev. B **61** (2000) 5571.
[11] T. U. Schulli, J. Stangl, Z. Zhong, R. T. Lechner, M. Sztucki, T. H. Metzger, and G. Bauer, Phys. Rev. Lett. **90**, 066105 (2003).
[12] V. Chamard, T. Schulli, M. Sztucki, T. H. Metzger, E. Sarigiannidou, J.-L. Rouviere, M. Tolan, C. Adelmann, and B. Daudin, Phys. Rev. B **69**, 125327 (2004).
[13] T. H. Metzger, T. U. Schulli, and M. Schmidbauer, C. R. Phys. **6**, 47 (2005).
[14] J. M. Cowley, *Diffraction Physics* (Elsevier Science Publishers B.V., Amsterdam, The Netherlands, 1986).
[15] See, e.g., L. V. Azaroff, *Elements of X-ray Crystallography* (McGraw-Hill, New York, 1968).
[16] S. Grenier, M. G. Proietti, H. Renevier, L. González, J. M. García, J. M. Gerard, J. García *et al.*, Europhys. Lett. **57**, 499 (2002).
[17] Y. M. Niquet, C. Priester, C. Gourgon, and H. Mariette, Phys. Rev. B **57**, 14850 (1998).